

Temporal Laser Pulse Shaping for RF Photocathode Guns: The Cheap and Easy way using UV Birefringent Crystals

John G. Power^a and Chunguang Jing^b

^a High Energy Physics Division, Argonne National Laboratory, Argonne, IL 60439

^b Euclid Techlabs, LLC, 5900 Harper Rd, Solon, OH-44139

Abstract. We report experimental investigations into a new technique for achieving temporal laser pulse shaping for RF photocathode gun applications using inexpensive UV birefringent crystals. Exploiting the group velocity mismatch between the two different polarizations of a birefringent crystal, a stack of UV pulses can be assembled into the desired temporal pulse shape. The scheme is capable of generating a variety of temporal pulse shapes including: (i) flat-top pulses with fast rise-time and variable pulse duration. (ii) microbunch trains, and (iii) ramped pulse generation. We will consider two applications for beam generation at the Argonne Wakefield Accelerator (AWA) including a flat-top laser pulse for low emittance production and matched bunch length for enhanced transformer ratio production. Streak camera measurements of the temporal profiles generated with a 2-crystal set and a 4-crystal set are presented.

Keywords: Laser Pulse Shaping, Emittance, Photoinjector, Bunch Train

INTRODUCTION

The characteristics of electron bunches emitted from an RF photocathode gun are directly linked to the distribution of the laser pulse striking the photocathode. Therefore, the ability to control the transverse and temporal (longitudinal) laser distribution allows one to create a variety of useful electron bunch profiles. For instance, it is well known that the uniform cylindrical laser pulse shape (flat-top intensity distribution in both the transverse and longitudinal dimensions) produces a lower transverse emittance than the ordinary Gaussian laser pulse shape. However, the natural laser pulse shape in most PC drive lasers is tri-Gaussian so pulse shaping is needed. While it is relatively easy to generate a transverse flat-top laser distribution (e.g. using an overfilled iris) the temporal structure is more difficult to manipulate.

Over the last several years various temporal pulse shaping schemes have been used to achieve reasonable success in generating temporal flattops; yet there is always room for improvement. In general, all schemes can be categorized as either frequency domain or time domain. In the former temporal pulse shaping scheme, *spectral masking*, a device is placed in the Fourier Transform plane of a stretcher to moderate the amplitude and/or phase of the input light to produce the desired pulse shape [1, 2]. However, when this technique is applied in the IR the rise-time tends not to be preserved through the IR amplifiers and the harmonic generation process and is therefore limited to about 3 ps [3]. In addition, the frequency domain IR pulse shaper

tends to be complicated and expensive as it requires feedback from the UV pulse to optimize the "*spectral mask*" settings. The rise-time situation can be improved if the frequency domain IR pulse shaper is followed by an additional stage of frequency domain UV pulse shaping, but the insertion losses can be quite high when ~ 1 ps rise-time is desired. The later temporal pulse shaping technique, *temporal pulse stacking*, directly stacks Gaussian pulses in the UV into an approximate flat-top. The advantage here is that the rise-time can be sub-ps; limited only by the seed pulse length and dispersion in the optics. This technique has been accomplished in the UV by using a combination of half-wave plates and beamsplitting cube polarizers [4] and, similarly, in a Michelson Interferometer configuration [5]. The drawback to this system is that it has proven difficult to adjust and align in practice.

Due primarily to the complexity and expense of previous pulse shaping systems, many smaller RF photoinjector facilities do not perform temporal pulse shaping. Recently, birefringent crystals have been used for pulse shaping in the IR [6] and therefore suffer from rise-time limitations. In this paper, we present investigations into a simple, economical system based on UV birefringent crystals.

TEMPORAL WALK-OFF IN BIREFRINGENT CRYSTALS

Birefringent crystals are anisotropic materials that have different indices of refraction for the two different polarizations of the incident light. The ray that is polarized perpendicular to the optical axis of the crystal is called the *ordinary* (*o*) ray and the ray that is polarized parallel to the optical axis is called *extraordinary* (*e*) ray. The magnitude of the birefringence of the crystal is difference between the two indices, $\Delta n(\lambda) = n_e(\lambda) - n_o(\lambda)$, where $n_e(\lambda)$ and $n_o(\lambda)$ are the index of refraction of the *o* ray and the *e* ray. Empirical formulas for $n_e(\lambda)$ and $n_o(\lambda)$ are available from the manufacture. For α -BBO the Sellmeier equations (λ in μm) are

$$n_{o\alpha\text{-BBO}}(\lambda) = \sqrt{2.7471 + \frac{0.01878}{\lambda^2 - 0.01822} - 0.01354\lambda^2} \quad (1)$$

$$n_{e\alpha\text{-BBO}}(\lambda) = \sqrt{2.3174 + \frac{0.01224}{\lambda^2 - 0.01667} - 0.01516\lambda^2} \quad (2)$$

Temporal walk-off is the term used to describe the temporal separation (Δt) that develops as the *o* ray and *e* ray propagate through the crystal. This loss of temporal overlap is due to the difference in the group index of refraction seen by the two rays. A short laser pulse (high bandwidth) incident on a birefringent crystal will be split into two pulses separated in time due to the differences in group velocity. The separation is the product of the crystal length, L , and the group velocity mismatch (*GVM*),

$$\Delta t = L \left(\frac{1}{v_{ge}} - \frac{1}{v_{g0}} \right) \quad (3)$$

where $v_{go}(=c/n_{go})$ and $v_{ge}(=c/n_{ge})$ are the group velocities for the *o ray* and *e ray* respectively, c is the speed of light in vacuum, and n_{ge} and n_{go} are group index of refraction for the *e ray* and *o ray* respectively. (Note that the explicit dependence on λ will be dropped in the remainder of the paper). The group index n_g is given by,

$$n_g = n - \lambda \left(\frac{dn}{d\lambda} \right) \quad (4)$$

and can be evaluated for a given crystal using Eq. 1 and Eq. 2. Note that positive birefringence occurs when the group velocity of the *o ray* greater than that of the *e ray* ($v_{go} > v_{ge}$) or ($n_{ge} > n_{go}$). Using these definitions we can rewrite Eq. 3 as, $\Delta t = L(\Delta n_g / c)$ where $\Delta n_g = n_{ge} - n_{go}$ is the group birefringence. Comparing Eq. 3 and 4 we recognize the group velocity mismatch as,

$$GVM = \Delta n_g / c \quad (5)$$

and the temporal walkoff is given by

$$\Delta t = L * GVM \quad (6)$$

Birefringent Crystals in the UV

Temporal pulse stacking based on birefringent crystals was first demonstrated [7] using a calcite crystal and a frequency-doubled Nd:YAG laser ($\lambda = 532$ nm). In that experiment, the crystal had a large group birefringence, $\Delta n_g = 0.23$ at 532 nm. Using Eq. 4, we calculate $GVM = 0.76$ ps/mm for calcite.

The ideal crystal for the pulse stacking application is strongly birefringent (large Δn_g) and transparent at the wavelength of interest. The difficulty with temporal pulse stacking technique in the UV (AWA laser is 248 nm) is due to the shortage of transparent and strongly birefringent crystals. While calcite's group birefringence is sufficiently strong, $\Delta n_g = 0.47$ at 248 nm, it is not transparent in the UV. Fortunately, an examination of commercially available uniaxial crystals reveals two promising candidates: crystal quartz and α -BBO. The values for n_e and n_o were provided by the manufacturer, while the values for n_{ge} , n_{go} , Δn_g , and GVM were calculated using the equations in the previous section. While crystal quartz is slightly more transparent than α -BBO (90% vs. 80%), we chose to use α -BBO due to its larger GVM (0.180 vs. -0.957 ps/mm).

A BIREFRINGENT TEMPORAL PULSE STACKER

Temporal pulse stacking is the process of splitting a seed laser pulse into a train (or stack) of laser pulses separated in time but aligned collinearly. In this section, we

show how to use a birefringent-based *Temporal Pulse Stacker* (TPS) to stack a single Gaussian seed pulse into a temporally flat-top laser pulse shape.

In general, a TPS using N birefringent crystals will transform a single Gaussian pulse into a stack of 2^N Gaussian output pulses and then recombine them into the single desired pulse. (i.e. 2 crystals make 4 pulses, 3 crystals make 8 pulses, etc.) Consider a 2 crystal α -BBO-based TPS used to transform a Gaussian seed pulse of $\text{rms}=\sigma$ into a stack of 4 Gaussian pulses that approximate an overall flat-top (Fig. 1). Let input Gaussian pulse be linearly polarized in the vertical direction while the optic axis of crystal #2, of length L_2 , is tilted at a 45° angle relative to the vertical. For α -BBO (a negative uniaxial crystal), the e-ray (component parallel to the optic axis), will move ahead of the o-ray (component perpendicular to the optic axis) by the amount, Δt_2 for crystal length L_2 . In this case ($n_e < n_o$), the extraordinary axis is the fast axis. The 45° orientation creates equal intensity e-ray and o-ray. (Notice that the relative intensity between the two rays can be controlled by a simple rotation of the optic axis which leaves open the possibility for ramped pulse generation.) The two (intermediate) pulses emerging from crystal #2 are now themselves oriented at 45° to the vertical. The next crystal (crystal #1) has its optic axis oriented in the same direction as the input pulse; i.e. in the vertical. When the two intermediate pulses pass through crystal #1, they are each further divided into 2 more pulses separated by Δt_1 with crystal length L_1 , thus producing the 4 output pulses.

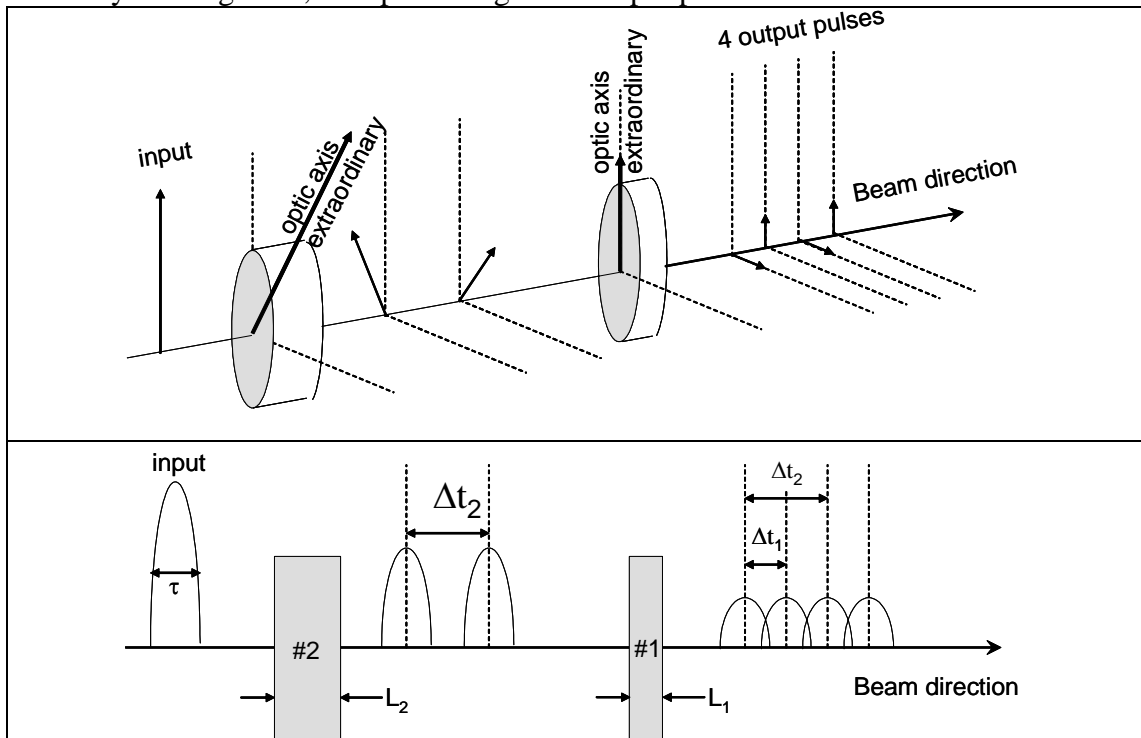


FIGURE 1. Schematic diagram showing 2 birefringent crystals used to produce 4 stacked Gaussians. (Top) The optic axis of the first crystal is oriented at a 45° angle relative to the input polarization while the optic axis of the second crystal is oriented in the same direction as the input polarization. (Bottom) The input pulse is split into two intermediate pulses, separated by Δt_2 , after the crystal of length L_2 . The intermediate pulses are further split and delayed by Δt_1 by the crystal of length L_1 to produce the 4 output pulses.

A Variety of Temporal Pulse Shapes

We now consider a few examples to illustrate the range of pulses that can be generated with an α -BBO-based TPS. In all cases we use a-cut, α -BBO crystals with $GVM = -0.957$ ps/mm at $\lambda = 248$ nm and ignore dispersion. The choice of a-cut means that there is no spatial walk-off since the optic axis is perpendicular to the direction of propagation. (Case 1) 2 crystals $L_1 = 6.5$ mm, $L_2 = 13$ mm; seed rms pulse length $\sigma = 3.5$ ps; output FWHM pulse length, $\tau = 24$ ps. (Case 2) 4 crystals $L_1 = 1.3$ mm, $L_2 = 2.6$ mm, $L_3 = 5.2$ mm, $L_4 = 10.4$ mm; seed rms pulse length $\sigma = 0.64$ ps; output FWHM pulse length, $\tau = 18$ ps. (Case 3) 4 crystals $L_1 = 4$ mm, $L_2 = 8$ mm, $L_3 = 16$ mm, $L_4 = 32$ mm; seed rms pulse length $\sigma = 0.64$ ps; output pulse separation, $\Delta\tau = 3.5$ ps. (Case 4) In this case, the crystals are not rotated as in Figure 1 but instead the first is rotated to 53° (not 45°) and the second is rotated to 3° (not 0°). This produces the ramped pulse shown in Fig. 2d.

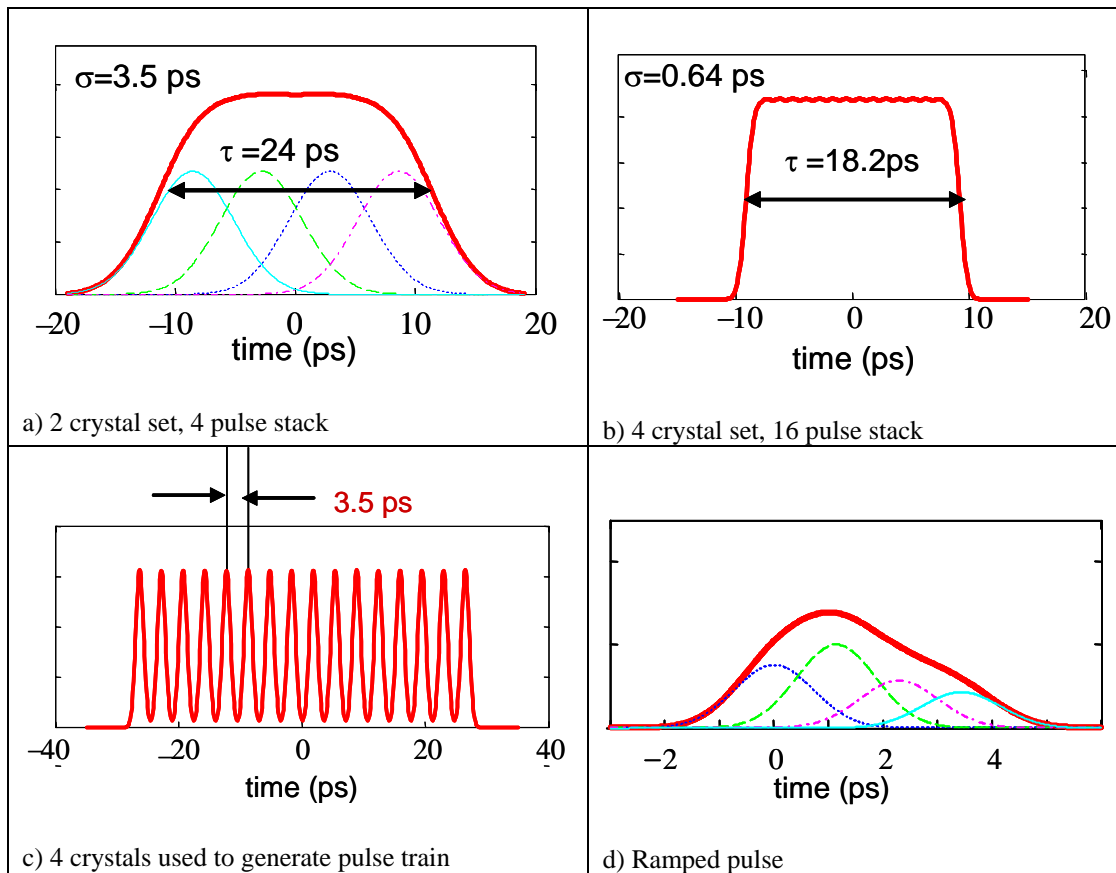


FIGURE 2. Output pulses that can be generated with an α -BBO-based TPS.

INITIAL RESULTS

Driven by the needs of two upcoming experiments at AWA, we ordered two sets of crystals: one set to produce a super-Gaussian pulse of $FWHM = 25$ ps (Case 1 above) and a second set to produce a flat-top of $FWHM = 18$ ps (Case 2 above). Streak

camera (Hamamatsu C1587) measurements for the examples are shown in Fig. 3a and Fig. 3b and should be compared directly to Fig. 2a and Fig. 2b. The measurements reveal partial success in generating the desired temporal shape, but there is significant modulation on the order of $\pm 20\%$. This is suspected to be due to a combination of improper setting of the crystal rotation angles and/or the wrong seed pulse length.

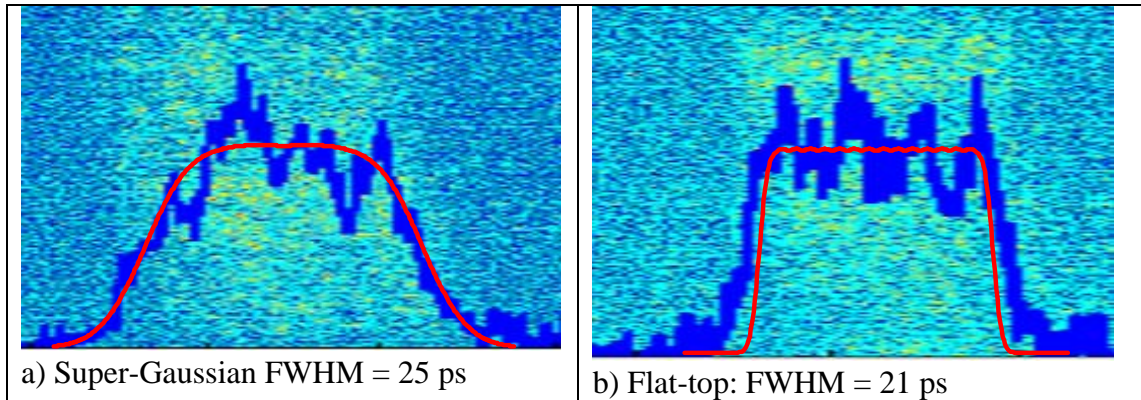


FIGURE 3. Streak camera measurement of output pulses.

CONCLUSIONS

In this paper, we investigated a new technique of *temporal pulse stacking* based on UV birefringent crystals [3, 4]. It has the advantage of being inexpensive and simple with a fast rise-time, but has the drawback of not being as flexible as frequency-domain schemes since the fixed length of the crystal sets the temporal structure. Future investigations will attempt to reduce the temporal modulation by more careful control of the rotation angle. In addition, we will study the possibility that the crystals are generating transverse stripes on the laser profile [8].

ACKNOWLEDGMENTS

One author (John Power) wishes to thank Yuelin Li for many useful conversations.

REFERENCES

1. Yang et al., *J. Appl. Phys* **92**, 1608 (2002)
2. F. Verluise et al., *J. Opt. Soc. Am. B* **17**, 138 (2000).
3. M. Petrarca et al., Proc. EPAC06, p. 3152 (2006); C. Vicario et al., Proc. PAC07, p. 1004 (2007);
4. S. Zhou et al., *Opt. Lett.* **32** (7), 871 (2007)
5. C. W. Siders et al., *Appl. Opt.* **37**, 22 (1998); M. Y. Shverdin, Proc. PAC07, p. 533 (2007)
6. <http://www.photonics.com/content/spectra/2007/May/research/87495.aspx>; B. Dromey et al., *Appl. Opt.* **46**, 22 (2007); S. Zhou et al., *Optics Letters*, **Vol. 32** No. 7, p. 871 (2007).
7. H. E. Bates, R. R. Alfano, and N. Schiller, *Appl. Phys. Lett.* **18**, 947 (1979).
8. T. Srinivasan-Rao, Private Communication